Biomedical Signal Processing and Control 44 (2018) 209–220

Contents lists available at ScienceDirect

Biomedical Signal Processing and Control

journal homepage: www.elsevier.com/locate/bspc

Divide-and-conquer muscle synergies: A new feature space decomposition approach for simultaneous multifunction myoelectric control

Gan Huang[a,b,c], Zhien Xian[a,b], Zhiguo Zhang[a,b,*], Shunchong Li[c], Xiangyang Zhu[c]

[a] School of Biomedical Engineering, Health Science Center, Shenzhen University, Shenzhen, 518060, China
[b] Guangdong Provincial Key Laboratory of Biomedical Measurements and Ultrasound Imaging, Shenzhen, 518060, China
[c] State Key Laboratory of Mechanical System and Vibration Shanghai Jiao Tong University, Shanghai, 200240, China

ARTICLE INFO

Article history:
Received 7 May 2017
Received in revised form 16 January 2018
Accepted 9 April 2018
Available online 8 May 2018

Keywords:
EMG
Feature space decomposition
Simultaneous control

ABSTRACT

Simultaneous multifunctional control based on surface electromyography (sEMG) is a key issue for natural and intuitive use of upper-limb prostheses in clinical and commercial applications. However, muscle synergies make simultaneous multifunctional control technologically challenging. In this study, we proposed a new feature space decomposition approach to alleviate the difficulty brought by muscle synergies for simultaneous control of hand and wrist movements. In the feature space decomposition approach, Gaussian mixture modeling (GMM) clustering is used to split the whole feature space into a set of Gaussian clusters, each consisting of samples with similar characteristics, to "divide-and-conquer" the complex muscle synergies. Then, a hybrid simultaneous control strategy, which consists of switch control of hand movements and proportional control of wrist movements, is performed in each cluster, instead of in the whole feature space. In the experimental study, sEMG signals were recorded during static and dynamic muscle contraction involving 2-dimensional wrist rotation (flexion-extension and radial-ulnar deviation) and 3 basic hand movement patterns (relaxing, fisting and grasping). Results show that, the new feature space decomposition approach can increase the accuracy for switch control of hand movement patterns from 90.10% to 96.62%, and can improve the correlation between true and predicted values of wrist rotation angular velocity from 0.71 to 0.84 (for wrist flexion-extension) and from 0.67 to 0.82 (for wrist radial-ulnar deviation) for proportional control of wrist. The proposed feature space decomposition approach has the potential to yield simultaneous multifunctional control for sEMG-based upper-limb prosthesis.

1. Introduction

Upper-limb prosthesis could largely increase the functional capacity of amputees and further improve their quality of life. Nowadays, surface electromyography (sEMG) is the main signal source to provide multifunctional control for upper-limb prosthesis [1–4], because it could be used with pattern recognition techniques to provide a natural mapping from upper-limb muscle motions to prosthesis functions with high accuracy and easy operation.

At present, the most common strategy for sEMG-based prosthesis is switch control, which means the output of the control system is switched among a certain number of pre-specified contraction patterns (usually 4–10 sustained hand and wrist postures). In the past decades, switch control has been proven to be a simple and robust control strategy. Most of the sEMG sensing systems based on the switch control can achieve response time shorter than 300 ms and recognition accuracy above 90% [5]. However, the switch control strategy is one major reason causing the non-intuitive control of prosthesis [6], because it can only provide a discrete univariate output and cannot recognize continuous variables (such as the velocity of wrist rotation) or control multiple joints, which is far from practical requirements of daily use [7,8].

A natural neuromuscular control of prosthesis should be proportional (i.e., to yield continuous outputs) and simultaneous (i.e., to produce multiple outputs for different joints at the same time). For upper-limb prosthesis, simultaneous proportional control has been realized for shoulder and elbow [9]. A hand grasping force estimation has also been included in the simultaneous proportional control of robots [10]. Some studies have investigated simultaneous

* Corresponding author at: School of Biomedical Engineering, Health Science Center, Shenzhen University, Shenzhen, 518060, China.
E-mail address: zgzhang@szu.edu.cn (Z. Zhang).

https://doi.org/10.1016/j.bspc.2018.04.011
1746-8094/

and proportional estimation of multiple degrees-of-freedom wrist movements for applications to myoelectric prosthesis control with amputations or congenitally deficient upper limbs [11–13].

However, simultaneous proportional control for wrist and finger motions still poses a great challenge, mainly because of the muscle synergies. Muscles of the forearm are distributed at three levels [14]: superficial, intermediate and deep. Flexors carpi radialis (FCR), flexors carpi ulnaris (FCU), extensor carpi radialis (ECR) and extensor carpi ulnaris (ECU) are layered in the superficial level of the forearm and they are most related to the flexion-extension of the wrist. Muscles related to the finger movement, such as flexor digitorum superficialis (FDS) and flexor digitorum profundus (FDP), are layered in the intermediate and deep levels of the forearm. As a consequence, it is difficult to isolate sEMG signals from each single muscle and to eliminate cross-talk from other muscles. Based on the hypothesis that behaviors might be produced through the combination of a small number of muscle synergies, several studies applied matrix factorization algorithms, like PCA, ICA, CSP, NMF, to identify relative activations between synergistic muscles for EMG-based prosthesis control.

- Principal Component Analysis (PCA) uses an orthogonal transformation to project the multi-channel EMG signal with the greatest variance on the first coordinate while the least variance in the data on the last coordinate. Hargrove et al. [15] used individual PCA to extract task-specific synergies so that the classification accuracy could be significantly improved.
- Independent Component Analysis (ICA) projects multi-channel EMG signal into statistically independent components. Staudenmann et al. [16] proved ICA could reduce the PCA-based predict error in muscle force estimation.
- Common Spatial Pattern (CSP) projects the signal to the new coordinate system with the aim of maximizing the difference in the variance between signal from two classes. Hahne et al. [17] demonstrated that CSP feature showed a high robustness against noise for myoelectric control.
- Non-negative matrix factorization (NMF) can decompose EMG signal into non-negative elements and it is another commonly used method for muscle synergies analysis [18–20].

Tresch et al. [21] compared the performance of PCA, ICA and NMF in identifying muscle synergies. It was found that PCA generally has lower performance than ICA and NMF, where ICA and NMF have comparable performance. In the comparison, the best algorithms were ICA applied to the subspace defined by PCA and a version of probabilistic ICA with nonnegativity constraints (pICA). It should be noted that all these blind source separation (BSS) methods are used on high-density EMG signal (HD-EMG) to identify time-invariant muscle synergies. It would be a challenge to identify time-variant muscle synergies from low-density EMG signal (LD-EMG). For LD-EMG, Huang et al. [22] embedded FIR filter in to CSP, which generates artificial channels with delayed signals and simultaneously filters in both the spatial and spectral domain to produce spectral features representing muscle synergies at particular spatial locations. For time-variant muscle synergies, wrist movements seriously interfere with the quality of sEMG signals from hand movements. During the wrist movements, the muscle synergies for hand movements would be time-variant, which makes the extremely difficult for by using BSS method. In [23], Reddy et al. showed the mutual influence for finger and wrist in their position estimation and applied a correction for the signal from FDS during wrist motion in their recognition model. They also showed that, the linear relationship between the wrist flexion-extension and the root mean square (RMS) of sEMG from FCU ($R^2 = 0.95$) was higher than that between finger position and the RMS of sEMG from FDS ($R^2 = 0.84$).

In the present study, we introduced a new feature space decomposition approach based on Gaussian mixture modeling (GMM) clustering to alleviate the difficulty brought by muscle synergies, and developed a hybrid simultaneous control strategy for both switch control of hand (i.e., to classify hand relaxing, fisting and grasping) and proportional control of wrist (to predict angular velocity of wrist rotation in the direction of wrist flexion-extension and radial-ulnar deviation). We designed a new experiment to record sEMG signals during a variety of static and dynamic hand and wrist movements involving wrist rotation and three hand patterns, and showed different patterns of muscle synergies in these hand/wrist movements. In the feature space decomposition approach, the GMM method groups samples into a finite number of clusters so that the samples in each cluster share similar characteristics in the feature space defined by time-domain (TD) sEMG features. We also investigated the distributions of TD features and showed that logarithm-transformed TD features are more Gaussian-like and thus are more suitable for GMM clustering. Next, the hybrid control strategy (including switch control of hand movements and proportional control of wrist movement) is performed for each cluster identified by GMM. For switch control of hand movements, a weighted Linear Discriminative Analysis (wLDA) classifier, which makes use of the prior probability of each cluster, to improve classification accuracy, is used; for proportional control of wrist movement, a multivariate linear regression (MLR) model is adopted. Experimental results show that the proposed feature space decomposition approach and hybrid simultaneous control strategy significantly improve the performance for both discrete classification of hand relaxing, fisting and grasping and continuous prediction of the angular velocity of wrist rotation in the direction of wrist flexion-extension and radial-ulnar deviation. Hence, the proposed feature space decomposition approach and hybrid control strategy can potentially make the prosthetic control more intuitive and reliable.

2. Materials and methods

2.1. Subjects

Eight subjects participated in this experiment (24.63 ± 4.27 years, 3 males 5 females). The sEMG signals were collected from their dominant arms (all subjects are all right handed). The experiments are in accordance with the Declaration of Helsinki. Ethical approval of the study was sought and obtained from the Bioethics Committee, School of Biomedicine Engineering, Shanghai Jiao Tong University (No. BM(E)2012045). Each subject was given the written informed consent prior to the experiment. No subject had a history of upper extremity or other musculoskeletal disorders.

2.2. Experimental procedures

To explore the role of muscle synergies, we compared the complex hand/wrist movements with pure hand movements in terms of the distributions of sEMG features and the performance in movement recognition. Fig. 1 illustrates the experimental setup. The experiment was carried out in 3 sections of hand and wrist movements: a dynamic section (10 min), a static section (3 min), and a repeated dynamic section (10 min). In each section, subjects were instructed to perform three types of hand movements alternately every 20 s, which were relaxing (all fingers relax), fisting (fingers flexed together in fist) and grasping (extension type grasp with a smartphone, 162 g of weight). In the static section, the subjects kept their wrists static. In the dynamic section, the subjects were asked to perform a full-amplitude wrist rotation in the clockwise direc-

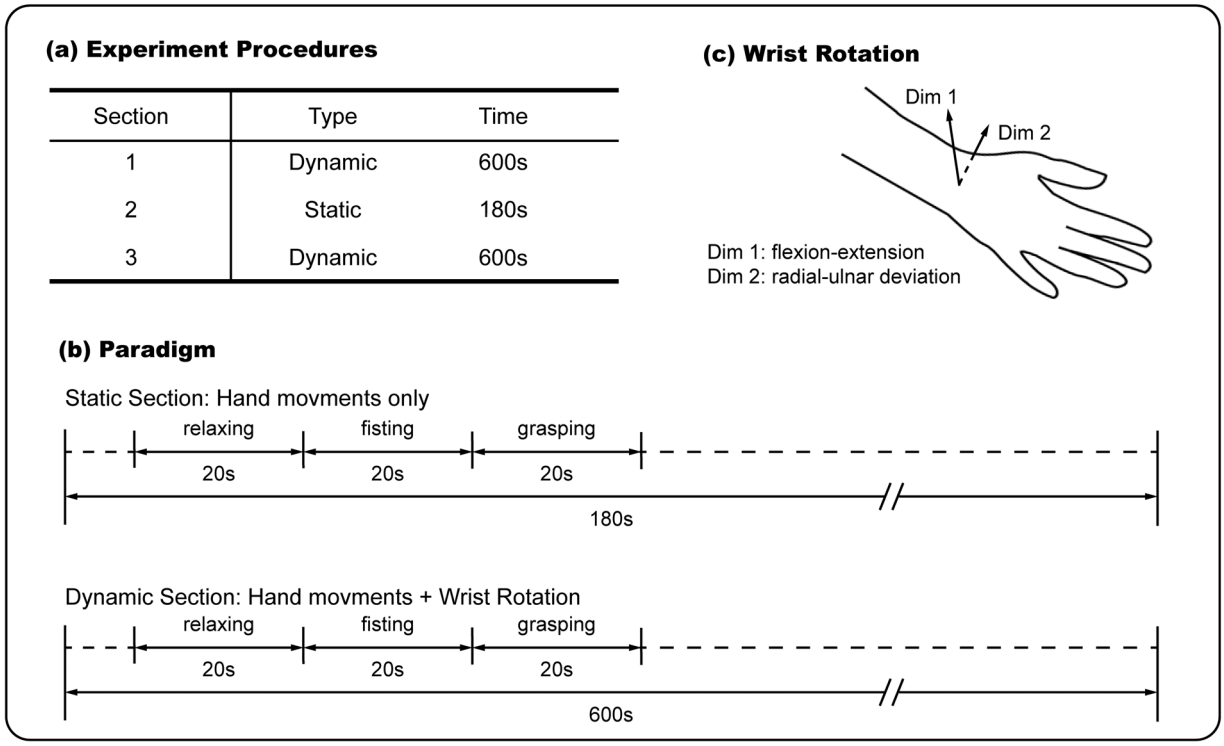

Fig. 1. Experiment setup. (a) The experiment consisted of three sections, which were one static section and two dynamic sections. (b) In the static section, the subjects kept their wrists static; in the dynamic section, the subjects were asked to perform a full amplitude wrist rotation. (c) The angular velocity for wrist rotation was derived and used for wrist movement recognition.

tion accompanied with the three types of hand movements that are the same as those in the static section. An animation of a rotating ball was displayed in the experiment to make sure all subjects follow the same rhythm. The rotation frequency of the ball varied in a frequency range from 0.6 Hz to 1.5 Hz, and this frequency range was determined by a pilot study. Some subjects reported feeling unnatural for a frequency below 0.6 Hz and some subjects were unable to follow the rhythm or felt tired for a frequency greater than 1.5 Hz.

2.3. Data collection

SEMG and angle signals were recorded simultaneously during the hand and wrist movements by Datalog-LS850 (Biometrics Ltd., Newport, UK). Six EMG sensors (SX320) were equally placed around the forearm in the correspondence to the radio humeral joint. A goniometer (SG65) was placed on the wrist to monitor the movement of wrist rotation in the dimensions of wrist flexion-extension and radial-ulnar deviation. The angular velocity for wrist rotation was derived and used for wrist movement recognition. Both sEMG and angle signals were sampled at 1000 Hz. It is important to note that, in this experiment only EMG sensors and goniometers are used, which are easy to be arranged. No further equipment is required to fix the hand or arm and to measure the torque as commonly conducted in related studies [24,25]. Hence, our training paradigm is more suitable for practical uses.

2.4. Method

In this study, a new feature space decomposition approach is proposed to alleviate the difficulty brought by muscle synergies for simultaneous control of hand and wrist movements, which includes three parts, which are 1) feature extraction, 2) feature space decomposition and 3) hybrid control (Fig. 2).

2.4.1. Feature extraction

A set of Time Domain (TD) features, including Mean Absolute Value (MAV), Wave Length (WL), Zero Crossing (ZC) and Slope Sign Changes (SSC), were extracted from sEMG for recognition of hand and wrist movements. TD features were originally proposed by Hudgins et al. [26], in which continuous sEMG signals were segmented into multiple frames and TD features were extracted from each frame. In [4], Englehart et al. used TD features for continuous sEMG control and they showed that the TD feature set was more powerful than other features, such as the wavelet packet features, for hand and wrist movement recognition. Due to the simplicity and effectiveness, the TD feature set is adopted in the present study. SEMG signals from 2 to 19 s for each relaxing, fisting and grasping motion were segmented into multiple samples with a window of 100 ms and an overlap of 75%. Note that the window length directly determines the response time for prosthesis control system. There are in total 6093 samples (677 samples per 20 s, 180 s) collected in the static section and 40620 samples (677 samples per 20 s, 1200 s). For each sample, there are 24 TD features (4 features per sensor, 6 sensors). MAV and WL are logarithmically transformed prior to the GMM clustering so that the log-transformed MAV and WL satisfy the Gaussian assumption of GMM (see details in Section 3A and Fig. 4). In the remaining part of this paper, we used TD to denote the feature set MAV, WL, ZC, SSC, and used log(TD) to denote the feature set log(MAV), log(WL), ZC, SSC. But ZC, SSC are not used for its singular in GMM clustering (more detail Sub-Section 2.4.2).

2.4.2. Feature space decomposition

To combat the problem of muscle synergies among the forearm muscles in the wrist and hand movement, GMM clustering is adopted to group all samples in the feature space into a small number of clusters. By the idea of “divide and conquer” [27], the GMM clustering algorithm can firstly “divide” the feature space into several clusters, then the recognition problem will be “conquered” in

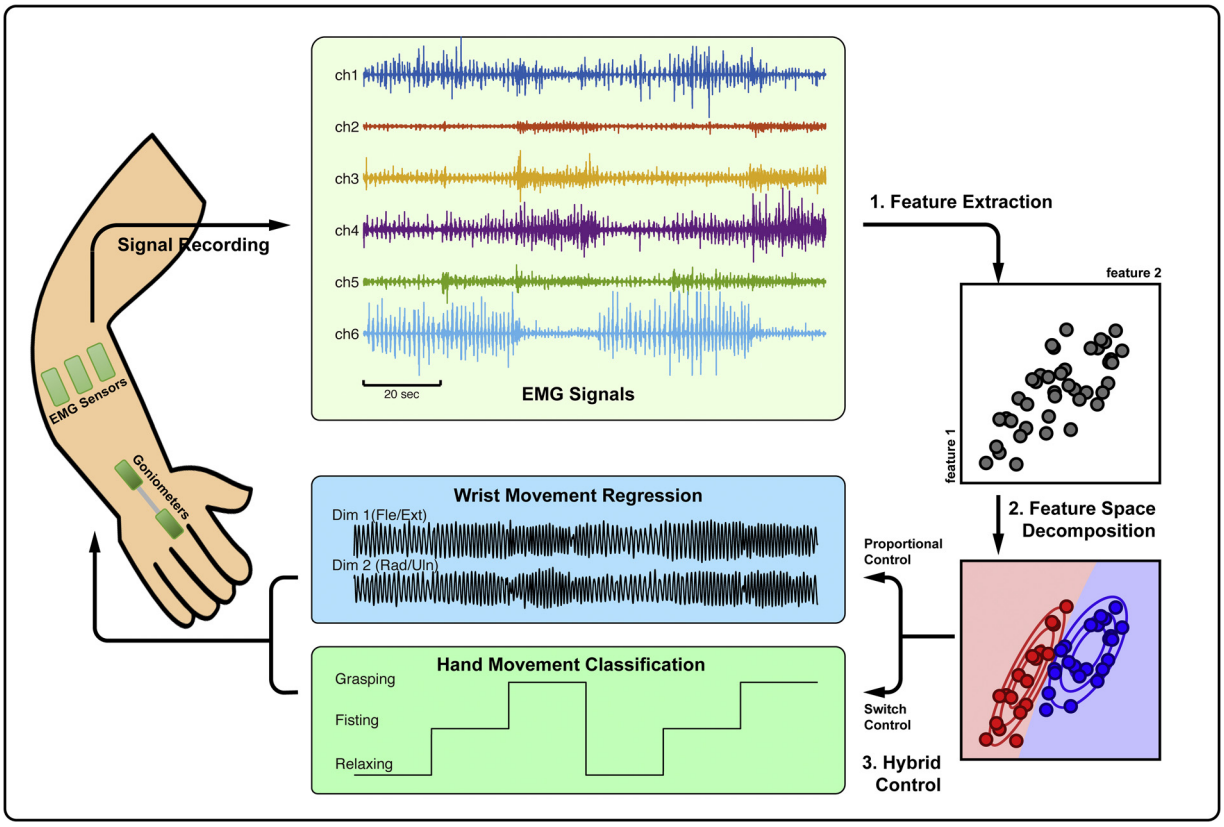

Fig. 2. Schematic diagram of the feature space decomposition approach and the hybrid control of hand.

each cluster, in which samples having similar features to ensure the classifier or the regression model is more specific. In this study, the "divide and conquer" strategy can recognize features in each cluster, where the state of wrist and hand movement shared similar characteristics, so that the recognition accuracy is expected to be higher than that achieved by recognition in the whole feature space. Among numerous clustering methods, GMM clustering is popularly used for its simple mathematical form and interpretability [28]. For continuous motion recognition, Panagiotis et al. [9,29], used a GMM based switching regime model to estimate arm motion for robotic control and the correlation coefficient between the estimation and real value for the Cartesian position of the user's hand in the 3-D space was increased by more than 0.1. Furthermore, GMM was also used as the classifier to recognize multiple upper-limb motions with the accuracy as high as 95.68% [30].

The Gaussian mixture model is described as a weighted sum of M Gaussian densities:

$$p(x) = \sum_{i=1}^{M} \omega_i g(x|\mu_i, \Sigma_i), \quad (1)$$

where $x \in \Re^D$ is the feature vector, for $i = 1, \ldots, M$, ω_i is the mixture weight and

$$g(x|\mu_i, \Sigma_i) = \frac{1}{(2\pi)^{D/2}|\Sigma_i|^{1/2}} \exp\left\{-\frac{1}{2}(x-\mu_i)'\Sigma_i^{-1}(x-\mu_i)\right\}, \quad (2)$$

is the D-dimensional Gaussian density function with mean vector μ_i and covariance matrix Σ_i. An expectation-maximization (EM) algorithm can be used to estimate the Gaussian distribution parameters (μ_i, Σ_i and ω_i) [31]. Each component (i.e., Gaussian density) is modeled as a specific cluster, and the cluster index for each sample is given by the component with the largest posterior probability, weighted by the component probability.

In this application, Gaussian mixture parameters (μ_i, Σ_i and ω_i for each cluster) are estimated from the features in the training stage. Then the clusters for both training and test features are constructed from the Gaussian mixture distributions. Subsequently, the classification (recognition of hand grasping and relaxing) or regression (recognition of the angular velocity of wrist flexion-extension) are performed in each cluster. Because the features ZC and SSC are positive integers with only a few (around 20) possible values, the estimate of the covariance matrix Σ_i in the GMM may become singular, especially when the number of components M is large and the number of samples in one component is very limited. Hence, only the features log(MAV) and log(WL) are used for GMM clustering

Fig. 3 illustrates the use of GMM based feature space decomposition approach for classification of hand relaxing and grasping. As seen from Fig. 3(a), the complex distribution of features makes a linear classifier over the whole feature space difficult to distinguish the two motions (the accuracy is 52.26%). In Fig. 3(b), by dividing the feature space into two clusters using GMM, samples of two hand motions can be better distinguished in each cluster (the accuracy is 81.82%).

To assess the structural difference of samples between the whole feature space and the clusters, the mean Standard Deviation (mSTD) of the possibility of three hand movement patterns in each cluster is calculated. For the classification of hand movement patterns, the standard deviation for cluster i can be calculated as

$$\mathrm{STD}_i = \sqrt{\frac{1}{3-1}\sum_{k=1}^{3}\left(p_k(i) - \frac{1}{3}\right)^2}, \quad (3)$$

where $p_k(i)$ is the probability of samples for each hand movement pattern in cluster i, k=1, 2, 3 corresponds to the hand movement patterns relaxing, fisting and grasping. If STD_i is close to 0, the number

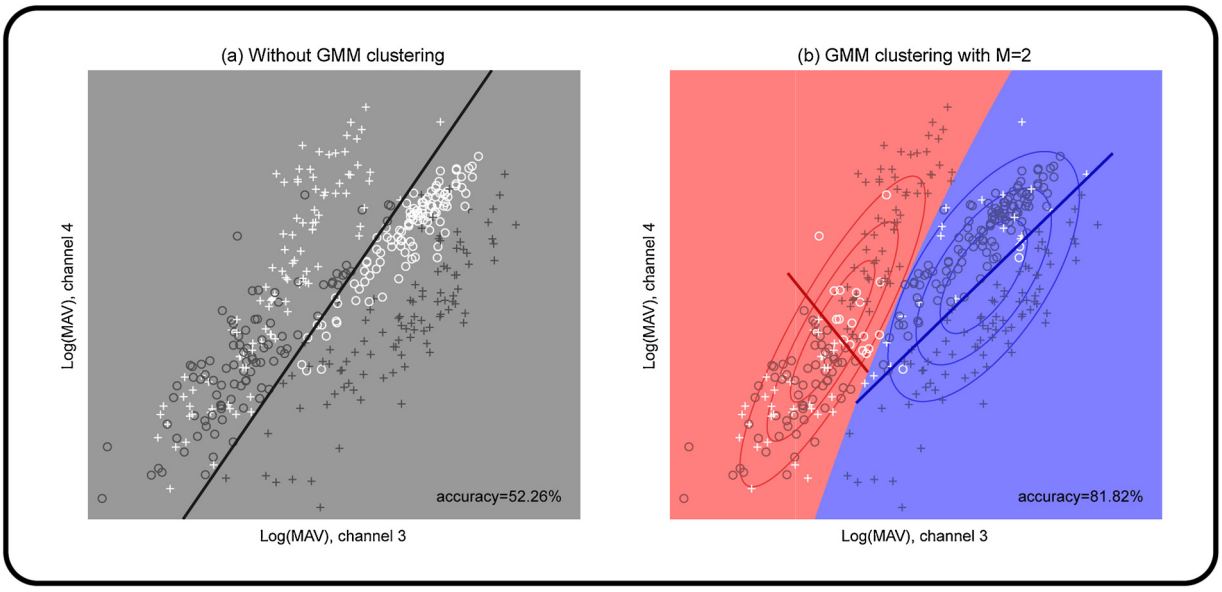

Fig. 3. An illustration of classification of hand grasping and relaxing without GMM clustering (a) and with GMM clustering (b). The features log(MAV) from two channels for hand relaxing (denoted as crosses) and grasping (denoted as circles) are used to illustrate the advantage of feature space decomposition by GMM clustering. Correctly classified samples and incorrectly classified samples are respectively marked with grey and white. The determinant functions of the classifiers are indicated by bold lines and the contour lines denote the Gaussian probability densities for each cluster. In (b), the number of components M is set to be 2.

of samples for three hand movement patterns in cluster i is almost equal and $[p_1(i), p_2(i), p_3(i)]$ will be close to [0.33,0.33,0.33]. If STD_i is close to 0.5774, the samples in cluster i are highly possible to belong to one of three hand movement patterns. For example, if the probabilities $[p_1(i), p_2(i), p_3(i)] = [1, 0, 0]$ in cluster i, $\mathrm{STD}_i = 0.5774$ according to Eq. (3). Based on STD_i, the quantity mSTD can be defined as follows:

$$\mathrm{mSTD} = \sum_{i=1}^{M} \frac{STD_i N_i}{N}, \tag{4}$$

where M is the number of the clusters used in GMM clustering, N_i is the number of samples in cluster i and N is the total number of samples. The value of mSTD ranges from 0 to 0.5774. A small mSTD close to 0 implies that the samples for the three hand movement patterns are almost equally distributed in every cluster. A large mSTD close to 0.5774 means the samples for the three hand movement patterns are distributed in different clusters, which is advantageous for pattern classification in each cluster.

2.4.3. Hybrid control

For hand movement recognition, a weighted LDA (wLDA) is used in both the static and dynamic sections to classify grasping and relaxing patterns. Linear Discriminative Analysis (LDA) [33] is a widely-used classifier for its simplicity (without any parameter selection). With the assumption that each class shares the same covariance matrix Σ, the discriminant function $g_c(x)$ for class μ_c is

$$g_c(x) = {\mu_c}^T \Sigma^{-1} x - \frac{1}{2} {\mu_c}^T \Sigma^{-1} \mu_c, \tag{5}$$

where μ_c is the mean value of class π_c and $c = 1, 2$ or 3, corresponding to the three hand patterns (hand relaxing, fisting and grasping). As a variant of LDA, wLDA further considers the prior probabilities $P(\pi_c)$ for class π_c in the discriminant function

$$g_c(x) = {\mu_c}^T \Sigma^{-1} x - \frac{1}{2} {\mu_c}^T \Sigma^{-1} \mu_c + \ln P(\pi_c), \tag{6}$$

Since GMM clustering can yield prior probabilities for the three motions in each cluster, the wLDA classifier can make use of such prior probabilities for a better classification performance. Therefore, wLDA, instead of LDA, is chosen as the classifier in this study. The classification accuracy of the hand relaxing, fisting and grasping is used as the criterion for assessing the performance of recognition of hand movement,

$$\mathrm{Accuracy} = \frac{\#\text{correctly classified samples}}{N} \times 100\%, \tag{7}$$

where N is the number of testing samples.

For recognition of wrist movement, the multivariate linear regression (MLR) method is used to predict the angular velocity of wrist rotation in both dimensions separately. For each testing sample x_i, the estimation of the wrist angular velocity $\hat{v}_i$ in one dimension is as follows,

$$\hat{v}_i = \alpha + \beta x_i, \tag{8}$$

The coefficients α and β could be computed by minimizing the sum of squared residuals

$$S(\alpha, \beta) = \sum_{j=1}^{L} \left(v_j - \alpha - \beta x_j\right)^2, \tag{9}$$

where v_j is the real angular velocity for training sample x_j, and L is the number of training samples. The R^2 value for one dimension

$$R^2 = 1 - \frac{\sum_{i=1}^{N} \left(\hat{v}_i - v_i\right)^2}{\sum_{i=1}^{N} \left(\hat{v}_i - \bar{v}\right)^2}, \tag{10}$$

is used for assessing the performance of the prediction, where $\hat{v}_i$ is the estimate of the real angular velocity v_i, and $\bar{v}$ represented the mean of v_i.

All the results come from the average of K-fold cross-validation, in which all the samples from each subject are divided into K parts and the training/testing procedure is repeated K times with each part as the testing samples and the remaining K-1 parts as training samples. K = 3 for the static section, in which all the hand motions are repeated 3 times, and K = 5 for the dynamic section, in which all the hand motions are repeated 20 times.

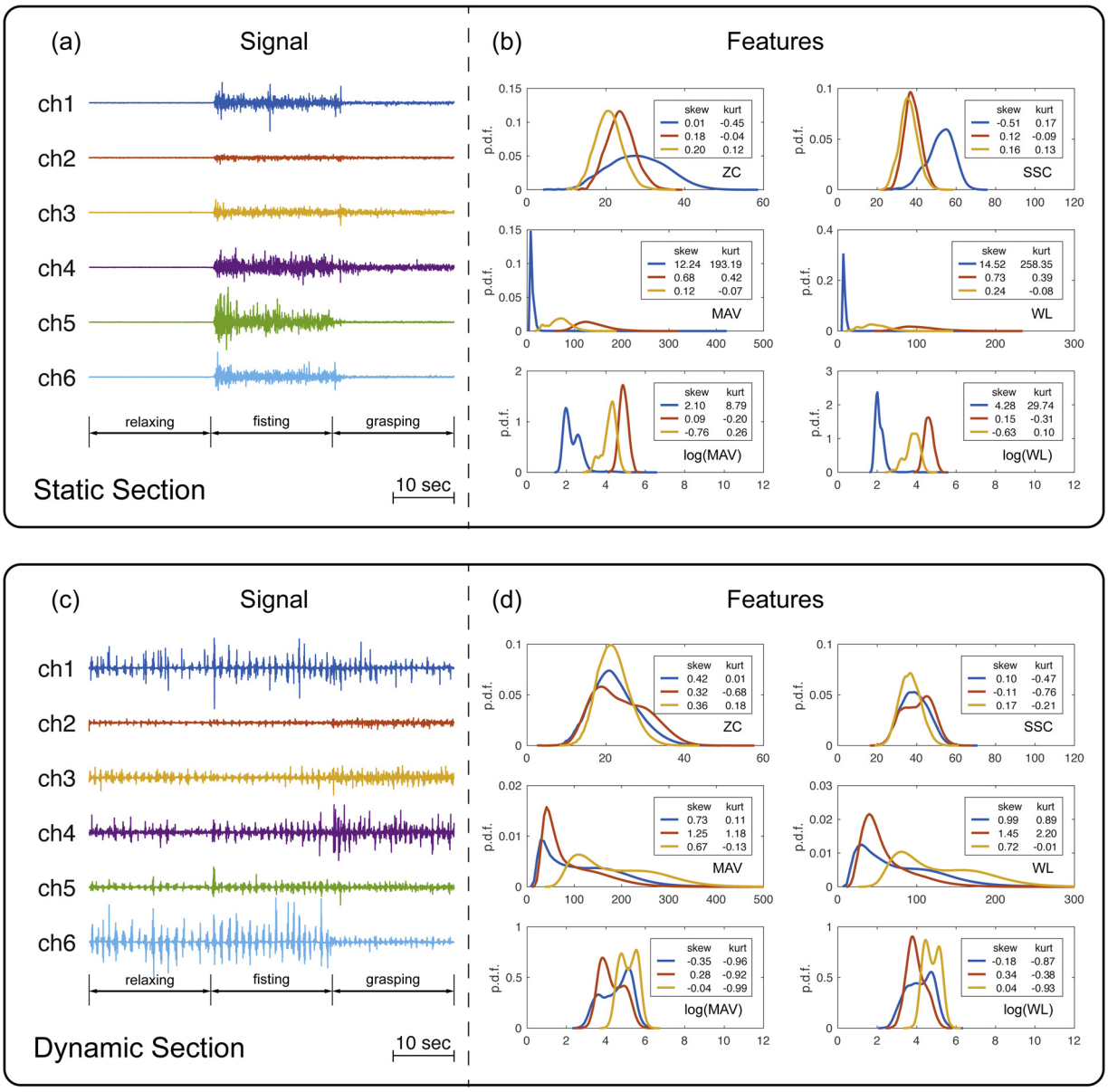

Fig. 4. Raw sEMG signals of one typical subject in the static session (a) and the dynamic session (c); the feature distributions and statistics (skew: skewness; kurt: kurtosis) of sEMG features from channel 3 for hand relaxing (blue lines), fisting (red lines) and grasping (yellow lines) in the static session (b) and the dynamic session (d). (For interpretation of the references to colour in this figure legend, the reader is referred to the web version of this article.)

3. Results

3.1. Gaussianity of sEMG features by muscle synergies

To illustrate the problem of muscle synergies in wrist and hand movements, raw sEMG signals and their feature distributions in both static and dynamic sections are shown in Fig. 4. In the static section, muscle synergies are task-specific. The activations between muscles related to hand and wrist movement are highly correlated. Hence in Fig. 4(a), hand fisting and grasping patterns can be easily identified from the large magnitudes of sEMG signals in different sensor channels. The remarkable difference in the distributions of TD features among hand relaxing, fisting and grasping makes it easy to distinguish the three hand movements (Fig. 4(b)). In the dynamic section, strong rhythmic sEMG signals related to wrist movement can be clearly observed at all channels, but the sEMG signals from hand grasping and relaxing are buried in the strong wrist-related sEMG signals and hard to be observed (Fig. 4(c)). Therefore, the difference between the feature distributions of hand relaxing, fisting and grasping in the dynamic section is not as obvious as it is in the static section (Fig. 4(d)), making the recognition of hand movements more difficult.

To check the Gaussianity of features, the skewness and kurtosis [34,35] for features MAV, WL, ZC, SSC, log(MAV) and log(WL) from one typical subject are labeled in Fig. 4(b) and (d). Furthermore, the mean absolute values of skewness and kurtosis for all these features are listed in Table 1. All the values are averaged from 6 sensors. The main observations of these TD features are as follows.

1. In the static section, MAV and WL for relaxing are smaller than those for fisting and grasping. The larger values of skewness and kurtosis indicate the stronger non-Gaussianity of MAV and WL for hand relaxing. In contrast, the MAV and WL features for fisting and grasping have smaller skewness and kurtosis, and thus are more Gaussian-like.
2. In the dynamic section, relaxing, fisting and grasping patterns share similar values of skewness and kurtosis for the dis-

Table 1
The skewness and kurtosis for features MAV, WL, ZC, SSC, log(MAV) and log(WL) for grasping and relaxing pattern in both static and dynamic sections. All the data are the mean absolute values from the 6 sensors of 8 subjects.

Section	Feature	Relaxing		Fisting		Grasping	
		Skewness	Kurtosis	Skewness	Kurtosis	Skewness	Kurtosis
Static	MAV	3.84	53.76	1.59	5.99	1.36	5.72
	WL	3.73	54.09	1.55	5.31	1.42	6.45
	ZC	0.02	0.13	0.15	0.02	0.17	0.04
	SSC	−0.15	0.19	0.04	−0.03	0.04	0.01
	log(MAV)	1.35	11.83	0.31	0.56	0.22	1.20
	log(WL)	1.52	16.03	0.36	0.55	0.27	1.49
Dynamic	MAV	1.63	4.41	1.53	4.10	1.57	8.51
	WL	1.73	4.95	1.42	2.98	1.64	10.24
	ZC	0.27	−0.17	0.18	−0.29	0.23	−0.00
	SSC	0.04	−0.13	−0.04	−0.14	0.01	−0.07
	log(MAV)V)	0.30	−0.36	0.10	−0.55	0.11	0.06
	log(WL)	0.36	−0.33	0.08	−0.62	0.15	0.27

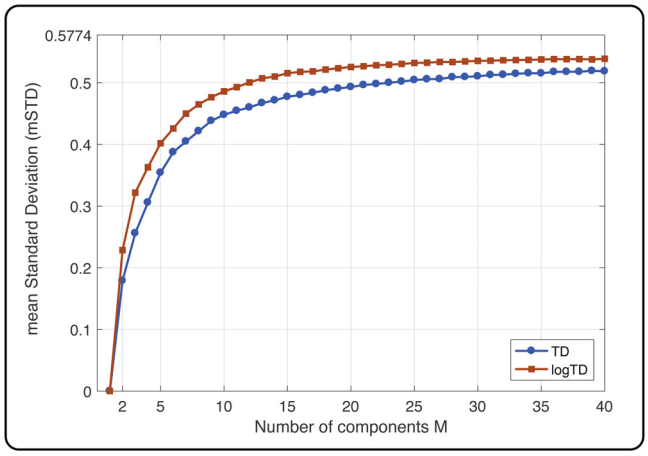

Fig. 5. The mean Standard Deviation (mSTD) for different number of clusters used in GMM clustering based on TD and log(TD) features.

tributions of MAV and WL, but they are not close to zero (i.e., less Gaussian-like). The skewness and kurtosis of the logarithm-transformed of MAV and WL are smaller, suggesting the logarithm transformation can substantially increase the Gaussianity of MAV and WL.

3. Compared with MAV and WL features, the distributions of features ZC and SSC have smaller values of skewness and kurtosis and are more Gaussian-like in both static and dynamic sections.

To sum up, the logarithmic operation on features MAV and WL could make the distributions of the two patterns more Gaussian-like (with much smaller skewness and kurtosis), and, therefore, more separable in the subsequent GMM based feature space decomposition.

The GMM based feature space decomposition approach is then used to partition samples into a small number of clusters. We first show in Fig. 5 that, the mSTDs for log(TD) features are higher than those for TD features, which means samples for hand grasping and relaxing can be better divided into different clusters by using log(TD) features. Subsequently, wLDA and MLR could make a better recognition in each cluster. It can also be seen from Fig. 5 that mSTDs for both TD and log(TD) features normally increase with M, which suggests that a larger M may lead to better recognition results.

3.2. Switch control of hand relaxing, fisting and grasping

Fig. 6 shows the classification accuracy for hand motions recognition in both static and dynamic sections. Considering the high accuracy (95.89% with TD features and 97.82% with log(TD) features) for static section, the GMM based feature space decomposition approach is only performed in the dynamic section with the number of mixture components M ranging from 2 to 40.

In the static section (Fig. 6(a)), the recognition accuracy of relaxing, fisting and grasping is $95.89 \pm 3.28\%$ with TD features. All subjects achieve an accuracy above 90%. The log(TD) features (with the accuracy of $97.82 \pm 1.99\%$) would further improve thre accuracy than TD features (with the accuracy of $95.89 \pm 3.28\%$), but there is no significant difference between the accuracies obtained using two types of features ($p = .074$, paired sample t-test). By using log(TD) features, two subjects (subject 5 and 6) have their accuracies decreased.

In the dynamic section (Fig. 6(b)), the accuracies for classification of hand movements are lower than those in the static section because of the muscle synergies caused by wrist movement. The accuracies of directly using TD and log(TD) features are $90.10 \pm 3.15\%$ and $92.83 \pm 4.57\%$ respectively. The improvement of log(TD) features over TD features is statistically significant ($p = .004$, paired sample t-test). As shown by the purple line in Fig. 6(b), only one subject (subject 2) has a decreased accuracy after the logarithm transformation.

Based on log(TD) features, the feature space decomposition approach could significantly improve the accuracy of hand movement recognition from $92.83 \pm 4.57\%$ (without GMM clustering) to $96.62 \pm 1.60\%$ with $M = 22$ ($p = .013$, paired sample t-test). As $M = 2$, the accuracy achieved by GMM clustering is $94.37\% \pm 3.39\%$, which is still better than the accuracy obtained without using GMM clustering with a substantial trend toward significance ($p = .012$, paired sample t-test). With the increase of M, the mean accuracy across all subjects increases and reaches the peak with $M = 22$. The mean accuracy for $M > 10$ is actually very stable. When M is larger than 30, the mean accuracy slightly decreases. For subjects with lower classification accuracies (such as subject 2), GMM clustering could greatly improve the accuracy. The accuracy for subject 2 is improved from 82.31% (without GMM clustering) to 93.62% (with GMM clustering $M = 25$).

By applying GMM clustering, mSTD is larger than 0.44 for both TD and log(TD) features with $M > 10$ (Fig. 5), which implies that the three hand patterns are easy to be distinguished in clusters. The wLDA classifier could make use of prior probabilities generated by GMM to improve the classification accuracy. As shown in Fig. 7, wLDA outperforms LDA for all M⟨*errorimage*⟩'s. With the increase of M, the accuracy with wLDA increases firstly and then slightly

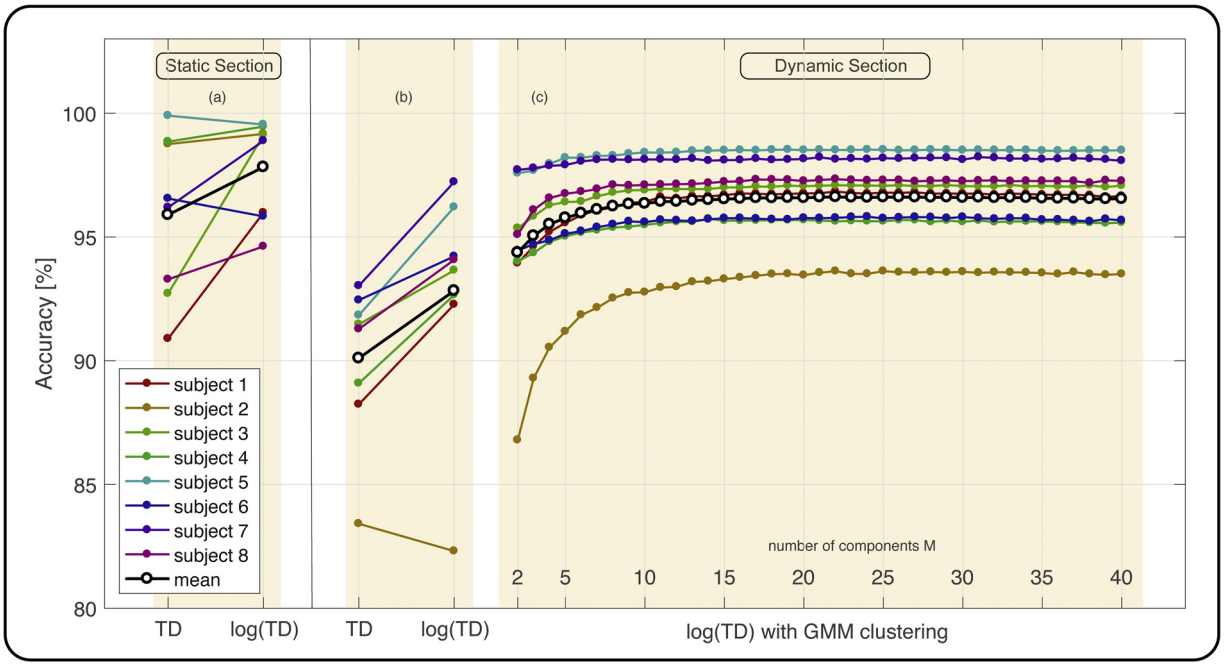

Fig. 6. The accuracy for the classification of hand grasping-relaxing in both static and dynamic sections. TD features include: MAV, WL, ZC and SSC; log(TD) features include: log(MAV), log(WL), ZC and SSC. Eight colored lines denote the accuracies of eight subjects. The black bold lines with circles are the averages of the eight subjects. In the dynamic section, only features log(MAV) and log(WL) are used for GMM clustering.

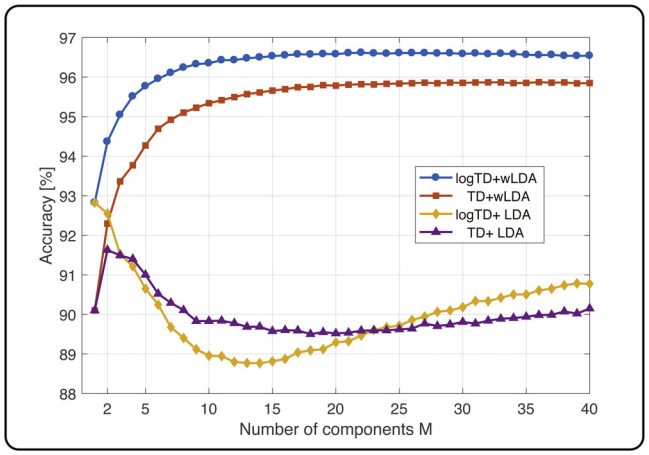

Fig. 7. Comparison of classification accuracy between using different types of features, TD or log(TD), and classifiers, LDA or wLDA, in the classification of hand relaxing, fisting and grasping.

decreases. For LDA, the performance decreases firstly and then increases with the growing of M. log(TD) features do not always outperform TD features, but they have the same trend with the increase of M. It should be noted that without the GMM clustering ($M = 1$), the number of hand relaxing, fisting and grasping samples have equal probabilities, and, thus, the wLDA is the same as LDA.

3.3. Proportional control of wrist angular velocity

For proportional control of wrist angular velocity, the results from GMM clustering method with log(TD) features are compared with the results obtained without using GMM clustering. To account for the interference of hand movement, the comparison is performed in two schemes. In Scheme 1 (as seen in Fig. 8), the wrist angular velocity in two dimensions are predicted separately during hand relaxing, fisting and grasping. The mean R^2 values for the three types of hand motions are compared in Scheme 1 (as seen in Fig. 8). In Scheme 1 (as seen in Fig. 8), the recognition is performed on the dataset consisting of all hand motions.

All the results are illustrated in Figs. 8 and 9 and Table 2, and can be summarized as follows.

1. GMM clustering based feature space decomposition approach can substantially improve the recognition accuracy. In Scheme 2 (as seen in Fig. 8), with GMM clustering, the R^2 values are significantly improved from 0.72 ± 0.05 to 0.84 ± 0.05 with $p < 10^{-6}$ in dimension 1 and 0.68 ± 0.03–0.81 ± 0.03 with $p < 10^{-5}$ in dimension 2. As the increase of M, the averaged R^2 values with log(TD) features increase from 0.76 ± 0.05 ($M = 2$) to 0.84 ± 0.05 ($M = 30$) in dimension 1 and 0.72 ± 0.03 ($M = 2$)–0.82 ± 0.03 ($M = 31$) in dimension 2. However, excessive components used in GMM clustering lower the R^2 values to some extent. With a larger number of M, the average number of training samples in each cluster would be small, which leads to the overfitting problem and makes the recognition results fall down. The results show the similar trends across all subjects.
2. GMM clustering based feature space decomposition approach could greatly alleviate the adverse influence of hand movements on wrist rotation. As listed in Table 2, the R^2 values in Scheme 2 (as seen in Fig. 8) for both TD and log(TD) features are lower than the corresponding results in Scheme 1 (as seen in Fig. 8). Without using GMM clustering method, the difference is significant (TD: $p < 10^{-6}$ in dimension 1 and $p < 10^{-5}$ in dimension 2, log(TD): $p < 10^{-4}$ in both two dimensions, paired sample t-test). By using GMM clustering in Scheme 2 (as seen in Fig. 8), the performance with TD features (0.82 ± 0.05 in dimension 1 and 0.79 ± 0.07 in dimension 2) is similar to the result in Scheme 1 (as seen in Fig. 8) (0.82 ± 0.05 in dimension 1 and 0.74 ± 0.03 in dimension 2) with no statistic significant ($p = .15$ in both dimensions, paired sample t-test); the performance with log(TD) features (0.84 ± 0.05 in dimension 1 and 0.81 ± 0.03 in dimension 2) is even better than the result in Scheme 1 (as seen in Fig. 8) (0.82 ± 0.05 in dimension 1 and 0.75 ± 0.03 in dimension 2) with statistic sig-

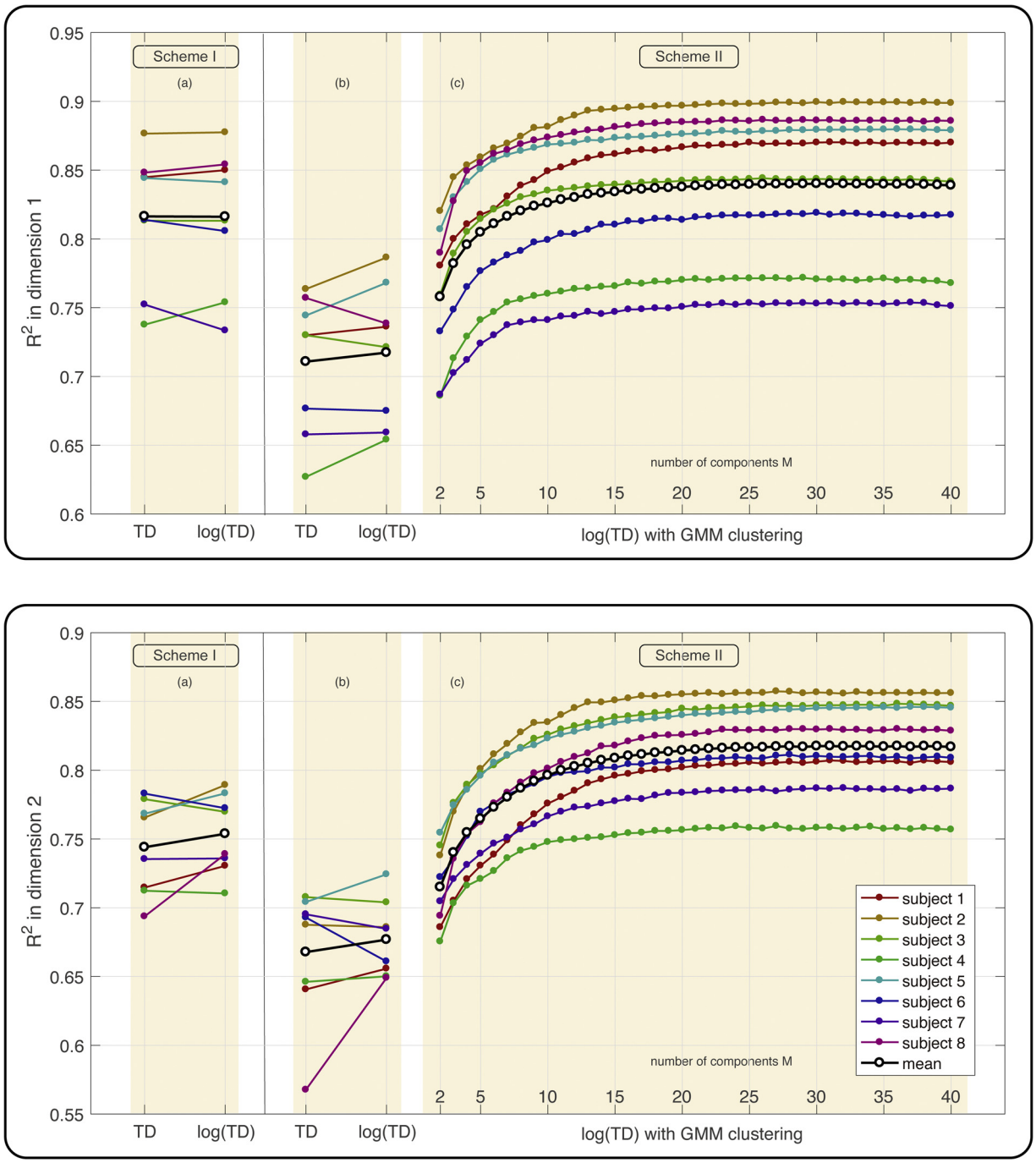

Fig. 8. The R^2 values for the prediction of angular velocity of wrist rotation in the two dimensions in both Schemes 1 and 2 (as seen in Fig. 8). TD features include: MAV, WL, ZC and SSC; log(TD) features include: log(MAV), log(WL), ZC and SSC. Eight colored lines denote the R^2 values of eight subjects. The black bold lines with circles are the averages of the eight subjects. In Scheme 2 (as seen in Fig. 8), only features log(MAV) and log(WL) are used for GMM clustering.

nificant ($p < 10^{-3}$ in dimension 1 and $p < 10^{-4}$ in dimension 2, paired sample *t*-test).

3. GMM clustering based feature space decomposition approach could make log(TD) features achieve better performance than TD features. By using GMM clustering, the R^2 values with TD and log(TD) features in dimension 1 and dimension 2 for different numbers of mixture components M are compared in Fig. 9. With the increase of *M*, the difference of the performance between log(TD) features and TD features also increases. The mSTD values in Fig. 5 suggest that the improved performance of log(TD) features over TD features may be ascribed to the better separation of three hand motions in each cluster by the GMM clustering.

3.4. Comparisons of classification and regression methods

To show the effectiveness of our method, we compare linear classifiers (LDA and wLDA) with nonlinear classifiers (including Quadratic Discriminant Analysis (QDA), weighted Quadratic Discriminant Analysis (wQDA), MultiLayer Perceptron (MLP), Support Vector Machine (SVM) and Naïve Bayes (Table 3), all of which are the common used methods in the hand movement classification. For wrist movement regression, we performed three regression methods: Multivariate Linear Regression (MLR), MLP and Support Vector Regression (SVR) (Table 4). All comparison is based on the log(TD) feature set, and the number of components in GMM is set

Table 2
The R^2 values of wrist movement recognition with different methods in both Schemes 1 and 2 (as seen in Fig. 8). Numbers in bold indicate the best results for both TD and log(TD) features in Dim1 and Dim2.

Comparison feature		Scheme 1	Scheme 2 without GMM clustering	Scheme 2 With GMM clustering(M=20)
Dim1	TD	0.82 ± 0.05	0.71 ± 0.05	0.82 ± 0.05
	log(TD)	0.82 ± 0.05	0.72 ± 0.05	$\mathbf{0.84 \pm 0.05}$
Dim2	TD	0.74 ± 0.03	0.67 ± 0.05	0.79 ± 0.07
	log(TD)	0.75 ± 0.03	0.68 ± 0.03	$\mathbf{0.81 \pm 0.03}$

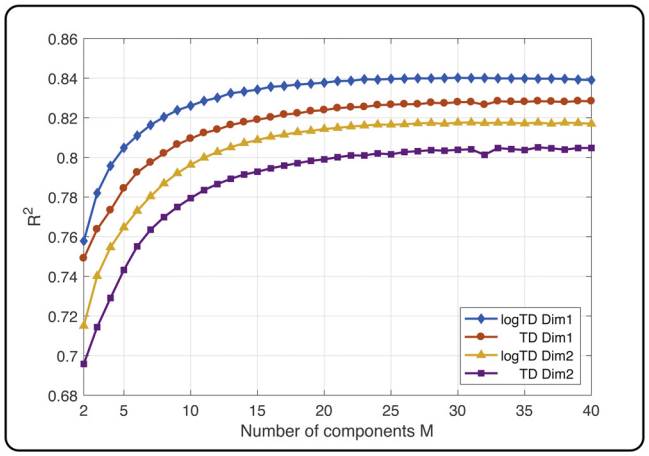

Fig. 9. Performance comparison of different types of features, TD or log(TD) used in the dynamic section of wrist movement recognition with GMM clustering.

to $M = 20$. For MLP, there is one hidden layer with 10 nodes and the activation function is the sigmoid function. For SVM in hand relaxing, fisting and grasping classification, RBF kernel function is used with gamma = 0.5; for SVR in wrist movement regression, linear kernel function is used. All the parameters are selected corresponding to the optimal results. In Table 3, it can be seen that in the static section, QDA (the same as wQDA) achieves better results that other methods. For the dynamic section, if feature space decomposition was not used, nonlinear methods achieved a better performance than linear methods in both classification and regression problems. Specifically, MLP performed better than other methods. After GMM clustering, linear methods were better than other methods under test. Specifically, wLDA performed better than LDA and other classifiers for switch control of hand movements, and MLR is better than other regression methods for proportional control of wrist movements.

It should be noted that the commonly used blind source separation (BSS) method for muscle synergies identifying would be not applicable for using here. That is because the muscle synergies for hand grasping and relaxing would not be time-invariance with the wrist movement, and also more EMG channels are needed to give full play to their advantages of these BSS methods. Some methods, like PCA, ICA and CSP could not identify hand grasping and relaxing effectively after blind source separation. Compared the NMF methods used in Ref. [6], the MSDSC-2 classifier achieves the best performance with 89.990% for hand grasping and relaxing recognition in the dynamic section.

4. Discussion and conclusion

Myoelectric control in upper arm prosthesis trends toward simultaneous multifunctional control. Detecting and refining the patterns of the muscle synergies play a crucial role in the success of the control scheme [36]. In this study, a feature space decomposition approach based on GMM clustering has been developed for decoding muscle synergies for switch control of hand relaxing, fisting and grasping and proportional control of the angular velocity of wrist rotation of upper-limb prosthesis. The novelty of this work is two-fold: the GMM clustering based feature space decomposition approach and the simultaneous hybrid control strategy.

First, the proposed GMM clustering based feature space decomposition approach could greatly overcome the common and serious challenges of muscle synergies during wrist and hand movements. For hand movement recognition, the mean classification accuracy was significantly increased from 90.10% (with TD features and without GMM) to 96.62% (with log(TD) features and with GMM) in presence of a full-amplitude wrist rotation, suggesting that the adverse influence of wrist movements on recognition of hand movements can be largely reduced by the proposed feature space decomposition approach. For wrist movement recognition, the proposed method increased the mean R^2 value from 0.71 for wrist flexion-extension and 0.67 for wrist radial-ulnar deviation (with TD features and without GMM) to 0.84 for wrist flexion-extension and 0.82 for wrist radial-ulnar deviation (with log(TD) features and with GMM). The use of GMM for clustering which is different from Ref. [22], in which the GMM is used as a classifier for the static hand guest. The results demonstrate that feature space decomposition could greatly eliminate the influence between the classification of hand motions and the recognition of wrist rotation and achieved better recognition accuracy. The reason is that, after feature space decomposition by GMM, each cluster consists of samples with similar characteristics, so that the complex mus-

Table 3
The accuracy for the classification of hand grasping-relaxing with LDA, wLDA, QDA, wQDA, MLP, SVM and Naïve Bayes.

Condition	LDA	wLDA	QDA	wQDA	MLP	SVM	Naïve Bayes
Static	97.82	97.82	**98.40**	**98.40**	97.00	96.99	96.93
Dynamic (no GMM)	92.83	92.83	94.88	94.88	**96.03**	93.42	80.41
Dynamic (GMM 20)	89.29	**96.58**	89.17	89.45	96.36	79.28	90.58

Table 4
The R^2 values of wrist movement recognition with MLR, MLP and SVR.

Condition		MLR	MLP	SVR
Dynamic (no GMM)	Dim1	0.7173	**0.8297**	0.7057
	Dim2	0.6768	**0.8067**	0.6291
Dynamic (GMM 20)	Dim1	**0.8377**	0.8199	0.8350
	Dim2	**0.8143**	0.7963	0.8107

cle synergies are simplified greatly. Selection of the number of clusters M is an important issue in GMM. Several different cluster validity algorithms, such as Silhouettes value [37] and Akaike criterion [38], could be used to determine the number of components, M. Based on our results, we suggest selecting 15–25 clusters in GMM (M = 15–25) for similar experiments. It should be noted that Gaussian mixture parameters estimation (μ_i, Σ_i and ω_i for each cluster) would be time consuming. In the offline 5-fold cross-validation, Gaussian mixture parameters estimation with the sample size 40620, feature dimension 24 on one subject will take less than 1.5 min with M = 2, close to 11 min with$M$ = 20, but almost 34 min with M = 40 (on the platform of MacBook Pro early 2015, macOS High Sierra, i5-2.9 GHz, 16G RAM, Matlab 2017b). While the Gaussian mixture parameters estimation is only performed in the training stage. Once the parameters μ_i, Σ_i and ω_i for each cluster is obtained, the speed for hand and wrist movement recognition in the testing stage is very fast. Hence it is available for the online myoelectric prostheses control.

Second, the hybrid control strategy has realized simultaneous recognition of wrist movement and hand grasping, which is more intuitive, effective and robust for daily applications. Considering the functional requirements for user acceptance of sEMG prosthesis [5], an ideal prosthesis should hold an object once grasping and prevent slipping, and also be able to provide a directly control of the velocity of wrist movements. The proposed control strategy can satisfy the above-mentioned functional requirements: it provide a robust and reliable control for hand grasping and makes users able to control the velocity of wrist movement. Hence, the hybrid control strategy could increase the user acceptance for prosthesis. The high performance (an accuracy >96% for recognition of hand relaxing, fisting and grasping and $R^2 > 0.82$ for recognition of wrist rotation) and the response time (100 ms) convincingly show the effectiveness and promptness of simultaneous multifunctional prosthesis control.

The present study can be extended in the future from the following four aspects.

1. To evaluate the feasibility of the proposed feature space decomposition approach and the simultaneous hybrid control strategy, only the simplest hand relaxing, fisting and grasping and wrist rotation in x-and y-axis are considered in this study. More types of hand and wrist motions, such as wrist supination and pronation, can be considered in future study. However, the hand and wrist motions are not independent: in some wrist angles, the hand motion could not be performed, and vice versa. Normally, more types of hand and wrist motions would decrease the classification accuracy. But it is still not clear whether wrist supination and pronation would lead to a more serious problem of muscle synergies and to what extent the hand recognition performance would be influenced by wrist supination and pronation or other wrist movements.
2. The performance of the proposed sEMG pattern recognition approach may be enhanced by increasing the response time (i.e., the length of analysis window for extracting sEMG features). A longer analysis window could provide a more accurate and stable estimate of sEMG feature and thus a higher performance, at the expense of a longer delay. Hudgins et al. stated that delays as long as 300 ms were not perceivable by users [4] and were not acceptable for prosthesis control. The window length used in this study is 100 ms, and it could be enlarged (up to 300 ms) for a better recognition performance, especially when there are more complex motions to be recognized.
3. In the pilot study for this experiment, we found one EMG sensor was not contacted well for around 10 s in our recording for two times, which will lead to a strong artifact. Normally, it will affect the recognition results seriously and the corresponding samples should be excluded from the training dataset. However, with the proposed GMM clustering based feature space decomposition approach, the samples with the artifact will be automatically separated into some special clusters, which alleviates the influence of the bad data for the recognition greatly. It will be interesting to explore how the clustering methods increase the robustness of the system against the influence of artifact in future.
4. It should also be pointed out that the goniometer was used in the experiment to record the velocity of wrist movements, which is unable to be used on amputees directly. Mirrored bilateral training [11,40] is an alternative approach to avoid this problem, in which the goniometer could be placed on wrist of the contralateral (mirrored) hand.

Acknowledgments

This work was supported by National Natural Science Foundation of China (No. 61701316), Research Project of State Key Laboratory of Mechanical System and Vibration (No. MSV201710), New Entry of teachers' scientific research project in Shenzhen University (No. 2018012), Shenzhen Peacock Plan (No. KQTD2016053112051497) and Science, Technology and Innovation Commission of Shenzhen Municipality Technology Fund (No. JCYJ20170818093322718). None of the authors have potential conflicts of interest to be disclosed.

References

[1] D. Graupe, W.K. Cline, Functional separation of EMG signal via ARMA identification methods for prosthetic control purposes, IEEE Trans. Syst. Man, Cybern. 5 (1975) 252–259.
[2] F.H.Y. Chan, Y.S. Yang, P.A. Parker, Fuzzy EMG classification for prosthesis control, History (2000) 1–9.
[3] M. Zecca, S. Micera, M.C. Carrozza, P. Dario, Control of multifunctional prosthetic hands by processing the electromyographic signal, Crit. Rev. Biomed. Eng. 30 (2002) 459–485.
[4] K. Englehart, B. Hudgins, A. Robust, Real time control scheme for multifunction myoelectric control, IEEE Trans. Biomed. Eng. 7 (2003) 848–854.
[5] B. Peerdeman, D. Boere, H. Witteveen, R.H. in 't Veld, H. Hermens, S. Stramigioli, H. Rietman, P. Veltink, S. Misra, Myoelectric forearm prostheses: state of the art from a user-centered perspective, J. Rehabil. Res. Dev. 48 (2011) 719–737.
[6] P. Pilarski, M. Dawson, T. Degris, Dynamic Switching and Real-time Machine Learning for Improved Human Control of Assistive Biomedical Robots, (BioRob), 2012, 4th 2012.
[7] M. Asghari Oskoei, H. Hu, Myoelectric control systems-A survey, Biomed. Signal Process. Control. 2 (2007) 275–294.
[8] D. Farina, S. Member, N. Jiang, H. Rehbaum, S. Member, The extraction of neural information from the surface EMG for the control of upper-limb prostheses: emerging avenues and challenges, IEEE Trans. Neural Syst. Rehabil. Eng. 22 (2014) 797–809.
[9] P.K. Artemiadis, K.J. Kyriakopoulos, An EMG-based robot control scheme robust to time-varying EMG signal features, IEEE Trans. Inf. Technol. Biomed. 14 (2010) 582–588.
[10] J. Vogel, C. Castellini, P. Van Der Smagt, EMG-based teleoperation and manipulation with the DLR LWR-III, IEEE Int. Conf. Intell. Robot. Syst. (2011) 672–678.
[11] J.L.G. Nielsen, S. Holmgaard, N. Jiang, K.B. Englehart, D. Farina, P.A. Parker, Simultaneous and proportional force estimation for multifunction myoelectric prostheses using mirrored bilateral training, IEEE Trans. Biomed. Eng. 58 (2011) 681–688.
[12] N. Jiang, J.L. Vest-Nielsen, S. Muceli, D. Farina, EMG-based simultaneous and proportional estimation of wrist/hand dynamics in uni-Lateral trans-radial amputees, J. Neuroeng. Rehabil. 9 (2012) 42.
[13] J.M. Hahne, F. Biebmann, N. Jiang, H. Rehbaum, D. Farina, F.C. Meinecke, K.-R. Muller, L.C. Parra, Linear and nonlinear regression techniques for simultaneous and proportional myoelectric control, IEEE Trans. Neural Syst. Rehabil. Eng. 22 (2014) 269–279.
[14] C.D. Clemente, Clemente's Anatomy Dissector: Guides to Individual Dissections in Human Anatomy with Brief Relevant Clinical Notes (applicable for Most Curricula), 2010.
[15] L.J. Hargrove, G. Li, K.B. Englehart, B.S. Hudgins, Principal components analysis preprocessing for improved classification accuracies in pattern-recognition-based myoelectric control, IEEE Trans. Biomed. Eng. 56.5 (2009) 1407–1414.

[16] D. Staudenmann, A. Daffertshofer, I. Kingma, D.F. Stegeman, J.H. van Dieën, Independent component analysis of high-density electromyography in muscle force estimation, IEEE Trans. Biomed. Eng. 54.4 (2007) 751–754.
[17] J.M. Hahne, B. Graimann, K.R. Muller, Spatial filtering for robust myoelectric control, IEEE Trans. Biomed. Eng. 59.5 (2012) 1436–1443.
[18] M.S. Shourijeh, T.E. Flaxman, D.L. Benoit, An approach for improving repeatability and reliability of non-negative matrix factorization for muscle synergy analysis, J. Electromyogr. Kinesiol. 26 (2016) 36–43.
[19] M. Silvia, N. Jiang, D. Farina, Extracting signals robust to electrode number and shift for online simultaneous and proportional myoelectric control by factorization algorithms, IEEE Trans. Neural Syst. Rehabil. Eng. 22.3 (2014) 623–633.
[20] S. Zhang, X. Zhang, S. Cao, X. Gao, X. Chen, P. Zhou, Myoelectric pattern recognition based on muscle synergies for simultaneous control of dexterous finger movements, IEEE Trans. Human–Mach. Syst. (2017).
[21] M.C. Tresch, V.C. Cheung, A. d'Avella, Matrix factorization algorithms for the identification of muscle synergies: evaluation on simulated and experimental data sets, J. Neurophysiol. 95.4 (2006) 2199–2212.
[22] G. Huang, Z. Zhang, D. Zhang, X. Zhu, Spatio-spectral filters for low-density surface electromyographic signal classification, Med. Biol. Eng. Comput. 51.5 (2013) 547–555.
[23] N.P. Reddy, V. Gupta, Toward direct biocontrol using surface EMG signals: control of finger and wrist joint models, Med. Eng. Phys. 29 (2007) 398–403.
[24] Z.O. Khokhar, Z.G. Xiao, C. Menon, et al., Surface EMG pattern recognition for real-time control of a wrist exoskeleton, Biomed. Eng. 9 (2010) 41, Online.
[25] A. Ziai, C. Menon, Comparison of regression models for estimation of isometric wrist joint torques using surface electromyography, J. Neuroeng. Rehabil. 8 (2011) 56.
[26] B. Hudgins, P. Parker, R. Scott, A new strategy for multifunction myoelectri control, IEEE Trans. Biomed. Eng. 40 (1993) 5541–5548.
[27] T. Cormen, R. Rivest, C. Leiserson, Introduction to Algorithms, 1989.
[28] B.S. Everitt, J. David, Hand, Finite mixture distributions, in: Monogr. Appl. Probab. Stat., Chapman Hall, London, New York, 1981.
[29] P.K. Artemiadis, K.J. Kyriakopoulos, A switching regime model for the emg-based control of a robot arm, IEEE Trans. Syst. Man, Cybern. Part B Cybern. 41 (2011) 53–63.
[30] Y. Huang, K. Englehart, B. Hudgins, A.D.C. Chan, A gaussian mixture model based classification scheme for myoelectric control of powered upper limb prostheses, IEEE Trans. Biomed. Eng. 52 (2005) 1801–1811.
[31] A.P. Dempster, N.M. Laird, D.B. Rubin, Maximum likelihood from incomplete data via the EM algorithm, J. Royal Stat. Soc. Ser. B 39 (1977) 1–38.
[33] R.O. Duda, P.E. Hart, D.G. Stork, Pattern Classification, 2001.
[34] K. Nazarpour, A.R. Sharafat, S.M.P. Firoozabadi, Surface EMG signal classification using a selective mix of higher order statistics, Eng. Med. Biol. Soc. 2005. IEEE-EMBS 2005. 27th Annu. Int. Conf. (2006) 4208–4211.
[35] K. Nazarpour, A. Al-Timemy, G. Bugmann, A. Jackson, A note on the probability distribution function of the surface electromyogram signal, Brain Res. Bull. 90 (2013).
[36] M. Ison, P. Artemiadis, The role of muscle synergies in myoelectric control: trends and challenges for simultaneous multifunction control, J. Neural Eng. 11 (2014) 51001.
[37] P. Rousseeuw, Silhouettes: a graphical aid to the interpretation and validation of cluster analysis, J. Comput. Appl. Math. 20 (1987) 53–65.
[38] H. Akaike, A new look at the statistical model identification, IEEE Trans. Automat. Contr. 19 (1974) 716–723.
[40] E.N. Kamavuako, D. Farina, K. Yoshida, W. Jensen, Estimation of grasping force from features of intramuscular EMG signals with mirrored bilateral training, Ann. Biomed. Eng. 40 (2012) 648–656.